ELSEVIER

Biochimica et Biophysica Acta 1511 (2001) 236–243

BIOCHIMICA ET BIOPHYSICA ACTA
BBA

www.bba-direct.com

Exclusion of a cholesterol analog from the cholesterol-rich phase in model membranes

Luís M.S. Loura [a,b], Aleksandre Fedorov [a], Manuel Prieto [a,*]

[a] *Centro de Química-Física Molecular, Instituto Superior Técnico, P-1049-001 Lisbon, Portugal*
[b] *Departamento de Química, Universidade de Évora, Rua Romão Ramalho 59, P-7000-671 Évora, Portugal*

Received 6 November 2000; received in revised form 20 December 2000; accepted 4 January 2001

Abstract

Vesicles of phosphatidylcholine/cholesterol mixtures show a wide composition range with coexistence of two fluid phases, the 'liquid disordered' (cholesterol-poor) and 'liquid ordered' (cholesterol-rich) phases. These systems have been widely used as models of membranes exhibiting lateral heterogeneity (membrane domains). The distributions of two fluorescent probes (a fluorescent cholesterol analog, NBD-cholesterol, and a lipophilic rhodamine probe, octadecylrhodamine B) in dimyristoylphosphatidylcholine/cholesterol vesicles were studied, at 30°C and 40°C. The steady-state fluorescence intensity of both probes decreases markedly with increasing cholesterol concentration, unlike the fluorescence lifetimes. The liquid ordered to liquid disordered phase partition coefficients K_p were measured, and values much less than unity were obtained for both probes, pointing to preference for the cholesterol-poor phase. Globally analyzed time-resolved energy transfer results confirmed these findings. It is concluded that, in particular, NBD-cholesterol is not a suitable cholesterol analog and its distribution behavior in phosphatidylcholine/cholesterol bilayers is in fact opposite to that of cholesterol.

Keywords: Model membrane; Cholesterol; Phase separation; Fluorescence; Energy transfer; Fluorescence resonance energy transfer; Partition; Fluorescent probe

1. Introduction

The detection and characterization of lipid microdomains is a major topic in membrane biophysics, because of their possible role in various biochemical functions [1]. While microscopic techniques with nanometer resolution are still under development, the most promising approaches to this problem are probably spectroscopic methods, such as photophysical techniques. These include measurement of fluorescence intensity, lifetimes and anisotropy [2], and time-resolved fluorescence resonance energy transfer (FRET). The latter has been used for the study of phase separation and domain formation in model membranes only very recently [3,4].

In this work, we studied dimyristoylphosphatidylcholine (DMPC)/cholesterol mixtures, which show phase separation of the liquid ordered (lo)/liquid disordered (ld) type, probably relevant to biological

Abbreviations: DMPC, dimyristoylphosphatidylcholine; FRET, fluorescence resonance energy transfer; LUV, large unilamellar vesicles; NBD-cholesterol, 22-(7-nitrobenz-2-oxa-1,3-diazol-4-yl-amino)-23,24-bisnor-5-colen-3β-ol; ORB, octadecylrhodamine B,

* Corresponding author. Fax: +35-1-218464455;
E-mail: prieto@alfa.ist.utl.pt

0005-2736/01/$ – see front matter
PII: S0005-2736(01)00269-3

membranes [5], using fluorescence techniques. The two probes used, 22-(7-nitrobenz-2-oxa-1,3-diazol-4-yl-amino)-23,24-bisnor-5-colen-3β-ol (NBD-cholesterol) and octadecylrhodamine B (ORB), form a donor/acceptor FRET pair. The NBD/rhodamine pair is a very common choice for FRET studies in membranes [3,6–10], and the use of a fluorescent sterol analog as donor and an acceptor bearing a long alkyl chain would in principle allow the study of phase separation in this system, similarly to a previous study in a gel/fluid heterogeneous system [4]. NBD-cholesterol is the most commonly used fluorescent analog of cholesterol, and has been used as such in numerous studies in the past (very recent examples being [11,12]). However, some reports have hinted at an unusual membrane distribution behavior of sterols labeled with a NBD moiety [13,14]. This prompted us to carry out a detailed spectroscopic study in this paper. Fig. 1 shows the lipid phase diagram (the studied systems are highlighted) and the probes' structures.

2. Materials and methods

NBD-cholesterol and ORB were purchased from Molecular Probes (Eugene, OR, USA). DMPC was obtained from Avanti Polar Lipids (Birmingham, AL, USA) and cholesterol was obtained from Merck (Darmstadt, Germany). All materials were used as received.

Preparation of the model membranes, large unilamellar vesicles (LUV), was carried out using the extrusion method [15]. Successful incorporation of ORB was achieved by injection of small amounts of methanol solution to previously prepared LUV [16], while for NBD-cholesterol small amounts of probe methanolic solution were mixed with the non-fluorescent lipid stock solutions in chloroform before hydration and extrusion, to ensure complete incorporation in the membranes.

The instrumentation for the fluorescence measurements has been described elsewhere in detail [4]. For NBD-cholesterol decays, excitation was at 340 nm and emission at 520 nm, while for ORB excitation was at 570 nm and emission at 610 nm. The goodness of fits to the decays was judged from the individual experiments' χ^2 values and weighted residuals and autocorrelation plots. Even in the absence of FRET, the observed decays were generally complex, and successful analysis required a sum of up to three exponential terms. Average lifetimes, $\langle\tau\rangle$, were calculated from [17]:

$$\langle\tau\rangle = \sum_i A_i \tau_i^2 / \sum_i A_i \tau_i \quad (1)$$

where τ_i are the decay lifetime components and A_i are their respective normalized amplitudes. Flu-

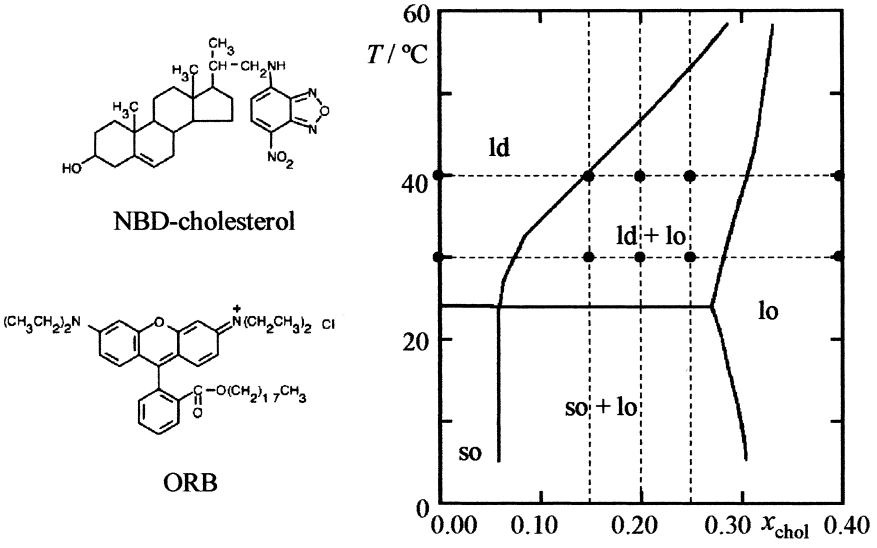

Fig. 1. (Left) Structures of the fluorescent probes used. (Right) DMPC/cholesterol phase diagram [5], highlighting the studied compositions and temperatures.

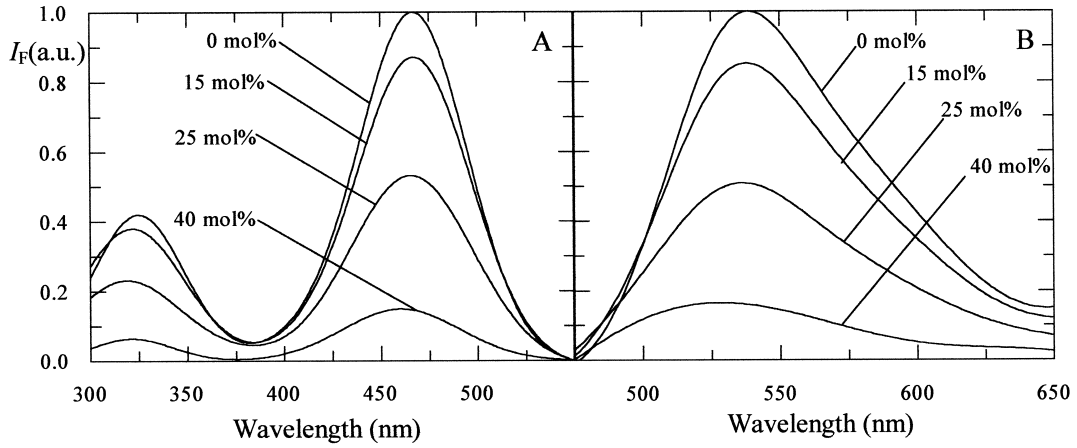

Fig. 2. Excitation (A; $\lambda_{emission} = 560$ nm) and emission (B; $\lambda_{excitation} = 334$ nm) spectra of NBD-cholesterol (0.1 mol%) in DMPC/cholesterol LUV, $T = 30$°C, for several cholesterol concentrations (indicated).

orescence steady-state measurements were carried out with a SLM-Aminco 8100 Series 2 spectrofluorimeter. Absorption spectra were measured in a Jasco V-560 spectrophotometer. Critical distances for energy transfer, R_0, were calculated from (e.g. [18]):

$$R_0 = 0.2108 \cdot \left[\kappa^2 \cdot \Phi_D \cdot n^{-4} \cdot \int_0^\infty I(\lambda) \cdot \varepsilon(\lambda) \cdot \lambda^4 \cdot d\lambda \right]^{1/6} \quad (2)$$

where Φ_D is the donor quantum yield, $\varepsilon(\lambda)$ is the acceptor molar absorption coefficient, κ^2 is the orientation factor, n is the refractive index (taken as 1.4, an average between the values in water and in the bilayer interior [19]), and λ is the wavelength. If the λ units used in Eq. 2 are nm, the calculated R_0 has Å units. The major source of uncertainty in the calculation of R_0 is often the orientation factor. In this work, we used $\kappa^2 = 2/3$, the dynamic isotropic limit value. Of course, the bilayer is not an isotropic medium. However, because the studied systems are composed of two fluid lipid phases, the dynamic limit is expected to be valid. This has been verified for lipophilic probes in the ld phase [16], and is also expected for the lo phase, in which the NBD-cholesterol fluorescence anisotropy is only slightly higher than in the ld phase (0.14 in the ld phase and 0.18 in the lo phase for $T = 40$°C). In this situation, κ^2 (and thus R_0) is expected to have an almost constant value for all donor–acceptor pairs.

3. Results

3.1. Probe photophysics

3.1.1. NBD-cholesterol

Fig. 2 shows the corrected excitation and emission spectra of NBD-cholesterol (0.1 mol%) in DMPC/cholesterol LUV at 30°C (identical trends were observed at $T = 40$°C). The most striking feature is the large decrease in fluorescence intensity with increasing cholesterol molar fraction, x_{chol} (by a factor of ~ 5 in the $0 \leq x_{chol} \leq 0.40$ range). Both excitation and emission spectra show a blue shift for high x_{chol}.

NBD-cholesterol shows complex fluorescence decays in DMPC/cholesterol LUV in the absence of ORB, and three lifetime components ($\tau_1 \sim 1$ ns, $\tau_2 \sim 4$ ns, $\tau_3 \sim 9$ ns) were needed to analyze most samples. At variance with the steady-state intensity, the maximum variation in $\langle \tau \rangle$ for the studied samples is relatively small ($\sim 5\%$; result not shown).

Fig. 3 shows the variation of fluorescence intensity (I_F) of NBD-cholesterol as a function of x_{chol}. This variation can be used to determine the lo to ld phase partition coefficient, K_p, defined as [2]:

$$K_p = (P_{lo}/X_{lo})/(P_{ld}/X_{ld}) \quad (3)$$

where P_{lo} is the probe molar fraction in the lo phase, and X_{lo} is the lo molar fraction (with $P_{ld} = 1 - P_{lo}$ and $X_{ld} = 1 - X_{lo}$ having an identical meaning for the ld phase). The relationship between I_F and the probe fraction within each phase for dilute samples (total

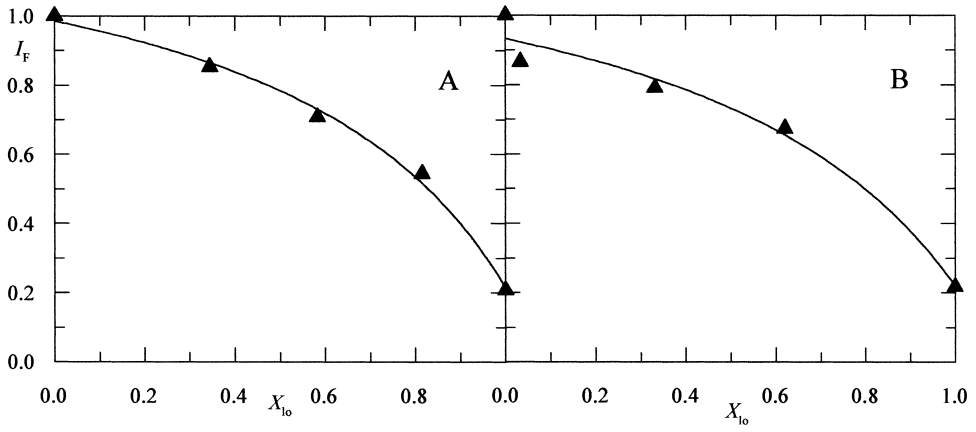

Fig. 3. Normalized fluorescence intensity (▲; $\lambda_{excitation} = 467$ nm, $\lambda_{emission} = 520$ nm) of NBD-cholesterol (0.1 mol%) in DMPC/cholesterol LUV, $T = 30$°C (A) and 40°C (B), as a function of the lo phase fraction (X_{lo}). The lines are fits using Eq. 4, with $K_p(30°C) = 0.35$ and $K_p(40°C) = 0.39$.

absorbance < 0.1) is given by (e.g. [4]):

$$I_F = K \cdot (P_{ld} \cdot \varepsilon_{ld} \cdot \Phi_{ld} + P_{lo} \cdot \varepsilon_{lo} \cdot \Phi_{lo}) \quad (4)$$

where K includes a geometric factor and the intensity of excitation light. Using $P_{lo}/P_{ld} = K_p \cdot (1 - X_{ld})/X_{ld}$, there are only two fitting variables, K and K_p. The solid curves in Fig. 3 were obtained in this way, $K_p(30°C) = 0.35$ and $K_p(40°C) = 0.39$ being recovered.

3.1.2. ORB

Fig. 4 shows the absorption ($T = 22$°C) and corrected emission ($T = 30$°C, similar results being observed for $T = 40$°C) of ORB (ORB:total lipid = 0.003) in DMPC/cholesterol LUV. For the absorption, the spectrum for a sample with the same bulk concentration in buffer is also shown for comparison. As observed with NBD-cholesterol, there is a significant reduction of absorption (~45%) and emission (~60%) intensities with increasing x_{chol} (from 0 to 0.4). While the emission spectrum is not shifted, the absorption maximum changes from 560 nm ($x_{chol} = 0$) to 565 nm ($x_{chol} = 0.4$). In any case, it is still far from the value observed in buffer (582 nm), where the absorption intensity is equal to that in pure DMPC (but there is an enhancement in the shoulder at ~540 nm, revealing excitonic interaction; this is absent from the LUV spectra). The emission in buffer (not shown) is ~20 times less intense

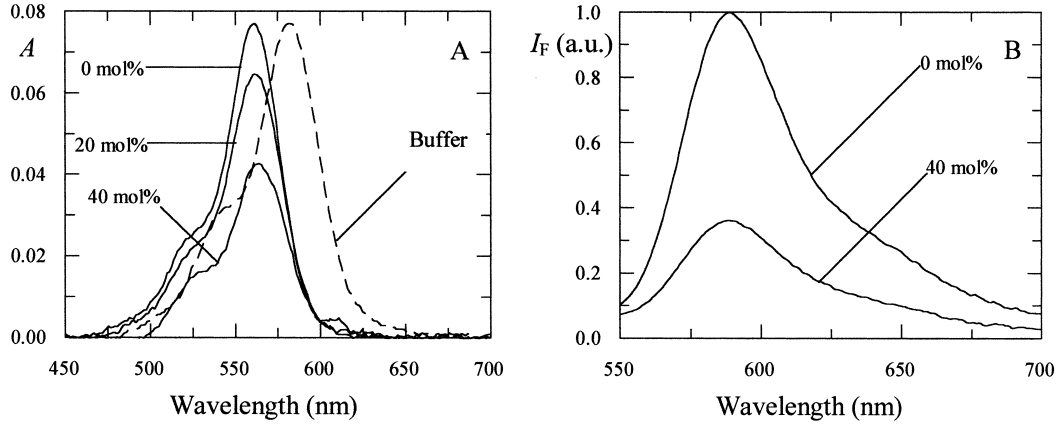

Fig. 4. Absorption (A; room temperature) and emission (B; $T = 30$°C; $\lambda_{excitation} = 515$ nm) spectra of ORB (0.3 mol%) in DMPC/cholesterol LUV, for several cholesterol concentrations (indicated).

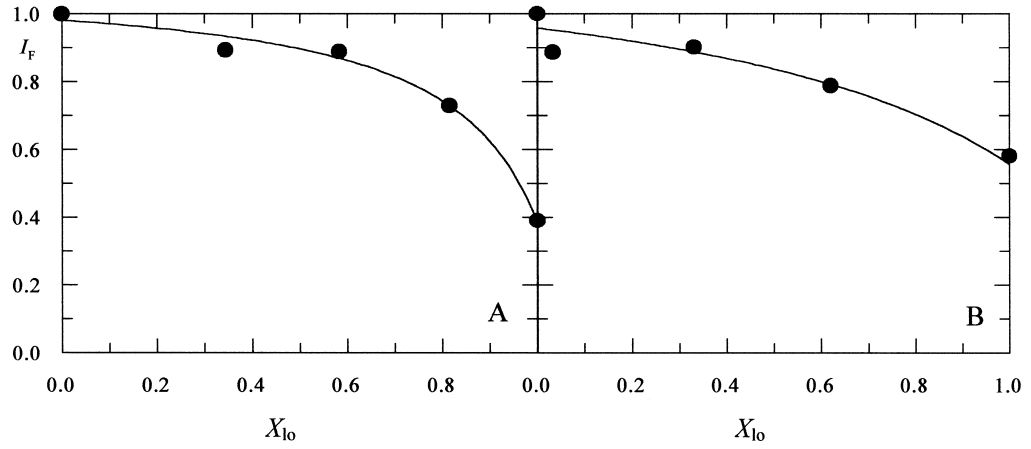

Fig. 5. Normalized fluorescence intensity (●; $\lambda_{excitation} = 560$ nm, $\lambda_{emission} = 593$ nm) of ORB (ORB:total lipid = 0.003) in DMPC/cholesterol LUV, $T = 30$°C (A) and 40°C (B), as a function of the lo phase fraction (X_{lo}). The lines are fits using Eq. 4, with $K_p(30°C) = 0.17$ and $K_p(40°C) = 0.43$.

than in pure DMPC, and has a maximum at ~619 nm, shifted 30 nm from the value observed in LUV.

Two exponentials are needed to analyze the ORB fluorescence decays for $0.0005 \leq$ ORB:total lipid ≤ 0.003 and $0 \leq x_{chol} \leq 0.4$. The average lifetime of ORB (ORB:total lipid = 0.0005) is almost constant as a function of x_{chol}, and equal to 2.2–2.3 ns at $T = 30$°C and 1.7 ns at $T = 40$°C. However, it decreases with increasing ORB concentration. For $x_{chol} = 0$, the relative decrease of $\langle\tau\rangle$ for $0.0005 \leq$ ORB:total lipid ≤ 0.003 is ~5%, while for $x_{chol} = 0.40$, and despite the smaller typical diffusion coefficients in the lo phase [5], which would lead to less dynamic self-quenching, the decrease is more pronounced (~15%; results not shown).

Similarly to NBD-cholesterol, K_p were obtained from the I_F variation using Eqs. 3 and 4, and the values $K_p(30°C) = 0.17$ and $K_p(40°C) = 0.43$ were recovered (see Fig. 5).

3.2. FRET between NBD-cholesterol and ORB

The critical distances for FRET, calculated from Eq. 2 using the spectroscopic parameters for these probes, are $R_0(30°C) = 44.8$ Å and $R_0(40°C) = 42.9$ Å. Due to the LUV preparation procedure, ORB is expected to be located on the outer monolayer, with its chromophore on the water region (~3.5 Å from the interphase, as determined by Medhage et al. [20] for another rhodamine lipophilic probe). On the other hand, the NBD-cholesterol chromophore should lie in the bilayer interior [21]. Thus, FRET bilayer geometry will be considered. In this way, the decay law used for analysis of FRET decay data was [4]:

$$i_{DA}(t) = i_D(t)\cdot[A_{ld}\cdot\rho_{ld}(t) + A_{lo}\cdot\rho_{lo}(t)] \quad (5)$$

where $i_D(t)$ is the decay law of NBD-cholesterol in the absence of ORB (taken as a sum of three exponentials), A_i is proportional to the amount of donors in phase i (i = ld, lo) and $\rho_i(t)$ is given by [19]:

$$\rho_i(t) = \exp\left\{-\frac{2c_i}{\Gamma(2/3)b}\int_0^1 [1-\exp(-tb^3\alpha^6)]\alpha^{-3}d\alpha\right\} \quad (6)$$

where c_i is proportional to the concentration of ac-

Table 1
Fit parameters of FRET decay data to Eqs. 5 and 6, in LUV of DMPC/cholesterol

T	Parameter	x_{chol}				
		0	0.15	0.20	0.25	0.40
30°C	c_{ld}	0.37	0.51	0.69	0.72	–
	c_{lo}	–	0	0.06	0.09	0.47
	A_{lo}/A_{ld}	0 (fixed)	0.18	0.64	0.76	∞ (fixed)
	χ^2	1.04	1.23	1.09	1.25	1.33
40°C	c_{ld}	0.45	0.61	0.63	0.64	–
	c_{lo}	–	0.01	0	0	0.54
	A_{lo}/A_{ld}	0 (fixed)	0.17	0.27	0.28	∞ (fixed)
	χ^2	1.28	1.20	1.22	1.24	1.50

Donor: NBD-cholesterol (0.1 mol%); acceptor: ORB (0.5 mol%).

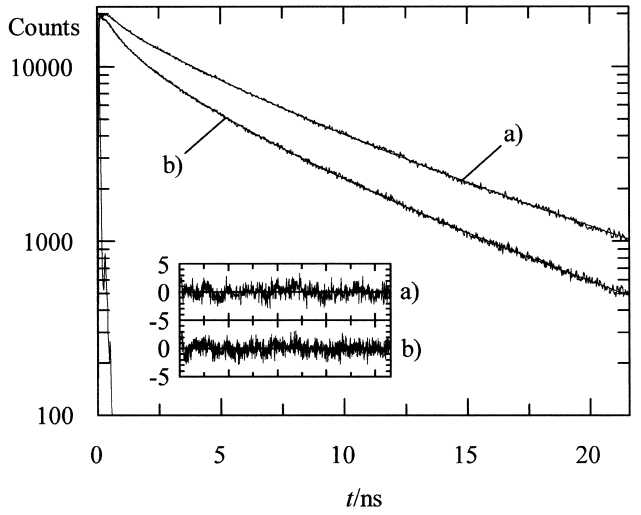

Fig. 6. Fluorescence decay curve of NBD-cholesterol (0.1 mol%) in LUV of DMPC/cholesterol ($x_{chol} = 0.20$) at $T = 30°C$. Also shown are the fitting curves (Eqs. 5 and 6) and the laser pulse profile. (Inset) Distributions of residuals. (a) no acceptor; (b): 0.5 mol% of ORB.

ceptors in phase i, and $b = (R_0/d)^2/\bar{\tau}$, where, in turn, d is the distance between the plane of donors and that of the acceptors (estimated as 17.8 Å [20,22]) and $\bar{\tau}$ is the lifetime-weighted quantum yield, given by $\Sigma A_j \tau_j$ [17]. Eq. 5 assumes that the donor decay is the same in both phases, which is a good approximation (see Section 3.1). Also assumed is that R_0 is equal for every donor–acceptor pair, which is a good approximation (see end of Section 2). The actual R_0 value is not crucially important, and its only effect is on the absolute values of the recovered c parameters (not their relative values). Thus small errors in R_0 (possibly arising from uncertainty in κ^2 and n in Eq. 2) are not critical for the discussion. Donor decays of samples containing no acceptor or 0.5 mol% ORB were analyzed together (global analysis [4,16]) for better recovery of parameters. The results of the analysis are shown in Table 1, and typical decay curves, fitting functions, and residuals distributions (for $x_{chol} = 0.20$, $T = 30°C$) are shown in Fig. 6.

For $x_{chol} = 0$, satisfactory fits are obtained fixing $A_{lo} = 0$ (as expected, being a fluid phase of a pure phospholipid [16]), and χ^2 improves non-significantly ($< 1\%$) when A_{lo} is optimized (not shown). However, for $x_{chol} = 0.40$, when a second c parameter is allowed, χ^2 improves by 7–17%, and one recovers an increased c (by $\sim 40\%$) and an additional c value of 0 (with $\sim 15\%$ relative weight; not shown). This indicates that, while for the ld phase the probe distribution is essentially random, this is no longer the case for the lo phase. The use of two c (c_{lo} and c_{ld}) parameters in analysis in the phase coexistence range ($x_{chol} = 0.15$, 0.20, and 0.25) also leads to ~ 10–20% improvement in χ^2, as expected for biphasic samples.

From the recovered A_i and c_i values it is possible to estimate the partition coefficients of donor and acceptor (respectively) between the two phases, as recently shown for a gel/fluid mixture [4]. The relevant equations for the K_p of acceptor (K_{pA}) and donor (K_{pD}) are:

$$K_{pA} = (c_{lo} \cdot a_{lo})/(c_{ld} \cdot a_{ld}) \quad (7)$$

$$K_{pD} = (A_{lo}/X_{lo})/(A_{ld}/X_{ld}) \quad (8)$$

where a_i is the average area per lipid molecule in phase i. These were calculated taking into account the bilayer condensation effect produced by cholesterol [23], together with the area per DMPC molecule in pure bilayers [22], and the values $a_{ld}(30°C) = 60.1$ Å^2, $a_{lo}(30°C) = 48.8$ Å^2, $a_{ld}(40°C) = 53.5$ Å^2, and $a_{lo}(40°C) = 45.2$ Å^2 were considered. Using Eqs. 7 and 8 and averaging for the three compositions inside the coexistence range, one obtains $K_{pA}(30°C) = 0.057$, $K_{pA}(40°C) < 0.01$, $K_{pD}(30°C) = 0.32$ and $K_{pD}(40°C) = 0.36$ (in this last value, the $x_{chol} = 0.15$ sample was not included, due to it being very close to the phase coexistence boundary, leading to large errors in X_{ld} and K_{pD} from Eq. 8).

4. Discussion

Quite interesting variations in photophysical parameters of both probes upon the addition of cholesterol were observed, and they can be rationalized by taking into account the properties of the NBD and rhodamine fluorophores. The hypsochromatic shift observed in NBD-cholesterol fluorescence spectra upon increasing x_{chol} is probably due to the reduction of permeability of the bilayer interior to water. The accessibility of the water molecules to the bilayer interior is drastically reduced upon increasing the cholesterol content [24,25]. The polarity of the NBD-cholesterol fluorophore microenvironment is thus reduced, leading to shorter maximal wave-

lengths [26,27]. The most striking feature, however, is the reduction in fluorescence intensity with increasing x_{chol}. This phenomenon, together with the relative invariance of $\langle\tau\rangle$, shows the existence of static self-quenching of this probe in the lo phase. The self-quenching of NBD fluorescence for very high local concentrations and/or aggregation is documented in the literature [28].

Contrary to NBD-cholesterol, the absorption spectrum of ORB shifts bathochromatically as x_{chol} increases (Fig. 4A). The maximum abscissa approaches the value in buffer, indicating that the chromophore becomes more solvated. This effect is probably due to steric restrictions caused by the cholesterol molecules, which act as spacers between phospholipid molecules, reducing their intermolecular interactions, and rendering their headgroups more accessible to the solvent [25]. On the other hand, the same phenomenon may be related to the excitonic interaction, apparent from the relatively enhanced shoulder in ORB absorption at $\sim$530 nm for high x_{chol}. The probable non-fluorescent nature of these aggregates explains the invariant fluorescence lifetime and emission maximum (on one hand) and the significant reduction of fluorescence intensity (on the other hand) upon increasing x_{chol}. The enhanced dynamic self-quenching of ORB measured for $x_{chol} = 0.40$ (where the diffusion is slower) relative to pure DMPC vesicles should be due to non-random ORB distribution in the lo phase.

Regarding the time-resolved FRET analysis, the results are compatible with the recovery of $K_p < 1$ for both probes from the I_F variation. In fact, for the acceptor, the concentration in the lo phase is always smaller than that in the ld phase ($c_{lo} < c_{ld}$). For the donor, it is clear that the ratio of molecules in the lo phase relative to those in the ld phase (given by A_{lo}/A_{ld}) is consistently < 1 (even when the lo phase is predominant, i.e. for $x_{chol} = 0.25$). The actual FRET K_{pD} values agree quantitatively with those of Section 3.1, but there is only qualitative agreement for K_{pA}. While both types of studies predict that ORB prefers the ld phase, the FRET data suggest complete ORB segregation for some samples. This results from the consistent recovery of a very small c value (often 0) in the phase coexistence range, and another larger than those of the monophasic samples (see Table 1). The fact that relative weight (given by A_{lo}/A_{ld}) of the FRET component characterized by $c \approx 0$ increases with x_{chol} allows its definite assignment to donors located in the lo phase. Thus, fluorescent donors in the lo phase are either isolated from acceptors or surrounded by a smaller acceptor local concentration. Note that due to the approximation made in the FRET analysis procedure (invariance of donor decay with x_{chol}), and despite the recovery of $c_{lo} = 0$ in some cases, one cannot state that these donors are definitely isolated, and that acceptors are completely segregated from the lo phase. In fact, in other samples $c_{lo} > 0$ is recovered. It is possible that one is not capable to distinguish $c_{lo} = 0$ from a situation characterized by a small (much smaller than c_{ld}) but finite c_{lo} value, due to the referred approximation.

In any case, the recovery of an isolated donor component indicates probe aggregation in the lo phase [29,30], in agreement with the studies in Section 3.1 (namely the reduction of fluorescence intensity). If the aggregates involve a large proportion of molecules and/or are located near ld/lo interphase regions (which is probable, given the molecules' preference for the ld phase), this aggregation will lead to a considerable rarefaction of probe molecules in the interior of the lo phase. Naturally, not all molecules aggregate in this phase, because I_F does not decrease to zero, even for $x_{chol} = 0.4$. The fluorescent donors in this phase would sense a reduced acceptor concentration that, under the FRET analysis approximations, could be confused with effective isolation.

The main conclusion from both the photophysical (Section 3.1) and FRET (Section 3.2) studies is that the probes aggregate significantly in the lo phase, which was not expected. Bearing in mind that NBD-cholesterol is commercialized as a fluorescent cholesterol analog, it would be reasonable to expect a priori that this probe would emulate the behavior of cholesterol, thus preferring the lo phase (from Fig. 1, one can estimate K_p(cholesterol, 30°C) ≈ 3 and K_p(cholesterol, 40°C) ≈ 2). However, this work allowed us to establish the inadequacy of this molecule to mimic cholesterol partition behavior in a phospholipid/cholesterol mixture (K_p(NBD-cholesterol) $\ll 1$). It agrees with recent reports that sterols labeled with a NBD moiety show anomalous distributions in living cells [13] and are excluded from cholesterol-rich vesicles [14]. The preference of NBD-

cholesterol for the ld phase is probably due to the bulky polar NBD group, which cannot be properly accommodated in a more tightly packed medium such as the lo phase. This is an important conclusion, and future research in phospholipid/cholesterol bilayers using photophysical techniques should use either sterols with larger structural similarity to that of cholesterol (such as dehydroergosterol [29,31], or the even more closely matched cholestatrienol [32]), or, subject to testing, head-labeled phospholipids which may not aggregate significantly in the lo phase. Fluorescence studies involving these kinds of probes in phospholipid/sterol systems are currently under way.

Acknowledgements

This work was supported by PRAXIS XXI (M.C.T., Portugal). A.F. acknowledges M.C.T. for financial support.

References

[1] O.G. Mouritsen, O.S. Anderson (Eds.), Topical issue: in search of a new biomembrane model, Biol. Skr. Dan. Vid. Selsk. 49 (1998) 1–214.
[2] L. Davenport, Methods Enzymol. 278 (1997) 487–512.
[3] W. Stillwell, L.J. Jenski, M. Zerouga, A.C. Dumaual, Chem. Phys. Lipids 104 (2000) 113–132.
[4] L.M.S. Loura, A. Fedorov, M. Prieto, Biochim. Biophys. Acta 1467 (2000) 101–112.
[5] P.F.F. Almeida, W.L.C. Vaz, T.E. Thompson, Biochemistry 31 (1992) 6739–6747.
[6] T.A.A. Fonteijn, J.B.F.N. Engberts, D. Hoekstra, Biochemistry 30 (1991) 5319–5324.
[7] J. Connor, A.J. Schroit, Biochemistry 26 (1987) 5099–5105.
[8] S.J. Eastman, J. Wilschut, P.R. Cullis, M.J. Hope, Biochim. Biophys. Acta 981 (1989) 178–184.
[9] G.W. Feigenson, Biophys. J. 73 (1997) 3112–3121.
[10] S. Pedersen, K. Jørgensen, T.R. Bækmark, O.G. Mouritsen, Biophys. J. 71 (1996) 554–560.
[11] C.N. Armah, A.R. Mackie, C. Roy, K. Price, A.E. Osbourn, P. Bowyer, S. Ladha, Biophys. J. 76 (1999) 281–290.
[12] O. Shatursky, A.P. Heuck, L.A. Shepard, J. Rossjohn, M.W. Parker, A.E. Johnson, R.K. Tweten, Cell 99 (1999) 293–299.
[13] S. Mukherjee, X. Zha, I. Tabas, F.R. Maxfield, Biophys. J. 75 (1998) 1915–1925.
[14] G.W. Feigenson, J. Huang, J.T. Buboltz, Biophys. J. 74 (1998) A201 (abstract).
[15] M.R. Hope, M.B. Bally, G. Webb, P.R. Cullis, Biochim. Biophys. Acta 812 (1985) 55–65.
[16] L.M.S. Loura, A. Fedorov, M. Prieto, Biophys. J. 71 (1996) 1823–1836.
[17] J.R. Lakowicz, Principles of Fluorescence Spectroscopy, 2nd edn., Kluwer Academic/Plenum Publishers, New York, 1999.
[18] M.N. Berberan-Santos, M.J.E. Prieto, J. Chem. Soc. Faraday Trans. 2 83 (1987) 1391–1409.
[19] L. Davenport, R.E. Dale, R.H. Bisby, R.B. Cundall, Biochemistry 24 (1985) 4097–4108.
[20] B. Medhage, E. Mukhtar, B. Kalman, L.B.-Å. Johansson, J.G. Molotkovsky, J. Chem. Soc. Faraday Trans. 88 (1992) 2845–2851.
[21] A. Chattopadhyay, E. London, Biochemistry 26 (1987) 39–45.
[22] D. Marsh, CRC Handbook of Lipid Bilayers, CRC Press, Boca Raton, FL, 1990.
[23] J.M. Smaby, M.M. Momsen, H.L. Brockman, R.E. Brown, Biophys. J. 73 (1997) 1492–1505.
[24] T. Parasassi, M. Di Stefano, M. Loiero, G. Ravagnan, E. Gratton, Biophys. J. 66 (1994) 763–768.
[25] P.L. Yeagle, W.C. Hutton, C. Huang, R.B. Martin, Biochemistry 16 (1977) 4344–4349.
[26] A. Chattopadhyay, E. London, Biochim. Biophys. Acta 938 (1988) 24–34.
[27] M.J.E. Prieto, M. Castanho, A. Coutinho, A. Ortiz, F.J. Aranda, J.C. Gómez-Fernandez, Chem. Phys. Lipids 69 (1994) 75–85.
[28] D. Hoekstra, Biochemistry 21 (1982) 1055–1061.
[29] L.M.S. Loura, M. Prieto, J. Phys. Chem. B 104 (2000) 6911–6919.
[30] L.M.S. Loura, A. Fedorov, M. Prieto, J. Phys. Chem. B 104 (2000) 6920–6931.
[31] L.M.S. Loura, M. Prieto, Biophys. J. 72 (1997) 2226–2236.
[32] P.A. Hyslop, B. Morel, R.D. Sauerheber, Biochemistry 29 (1990) 1025–1038.